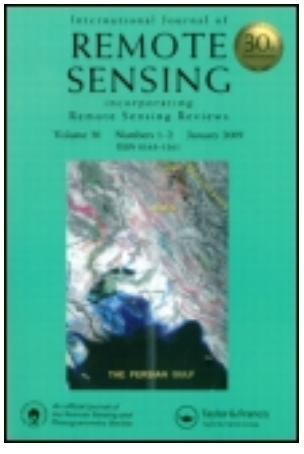


International Journal of Remote Sensing

Publication details, including instructions for authors and subscription information:
http://www.tandfonline.com/loi/tres20

# Eddy-feature phytoplankton bloom induced by a tropical cyclone in the South China Sea

Yongqiang Chen [a b c] & Danling Tang [a b]

[a] Research Centre for Remote Sensing of Marine Ecology and Environment (RSMEE), State Key Laboratory of Tropical Oceanography, South China Sea Institute of Oceanology, Chinese Academy of Sciences, Guangzhou, 510301, PR China

[b] Graduate University of the Chinese Academy of Sciences, Beijing, 100049, PR China

[c] Hainan Tropical Marine Biological Research Station, South China Sea Institute of Oceanology, Chinese Academy of Sciences, Sanya, 572000, PR China

Version of record first published: 10 Jul 2012

To cite this article: Yongqiang Chen & Danling Tang (2012): Eddy-feature phytoplankton bloom induced by a tropical cyclone in the South China Sea, International Journal of Remote Sensing, 33:23, 7444-7457

To link to this article: http://dx.doi.org/10.1080/01431161.2012.685976

*International Journal of Remote Sensing*
Vol. 33, No. 23, 10 December 2012, 7444–7457

Taylor & Francis
Taylor & Francis Group

# Eddy-feature phytoplankton bloom induced by a tropical cyclone in the South China Sea

YONGQIANG CHEN†‡§ and DANLING TANG*†‡
†Research Centre for Remote Sensing of Marine Ecology and Environment (RSMEE), State Key Laboratory of Tropical Oceanography, South China Sea Institute of Oceanology, Chinese Academy of Sciences, Guangzhou 510301, PR China
‡Graduate University of the Chinese Academy of Sciences, Beijing 100049, PR China
§Hainan Tropical Marine Biological Research Station, South China Sea Institute of Oceanology, Chinese Academy of Sciences, Sanya 572000, PR China

(*Received 29 December 2010; in final form 13 July 2011*)

This is the first report on an eddy-feature phytoplankton bloom induced by a tropical cyclone (the spiral structure of the bloom was coincident with that of a cold eddy) in the South China Sea (SCS). Applying satellite data, this report can furnish fresh evidence of the relationship between the bloom and the cold eddy. Tropical cyclone Linfa passed over the northern SCS from 16 to 21 June 2009. While it looped over for 2 days (from 17 to 19 June), a cold eddy, which lasted for 11 days in the looping area, was observed on 18 June. Subsequently, an eddy-feature phytoplankton bloom (central location: 18° N, 117.5° E) was detected on 22 June and it remained for 17 days. The character of both the cold eddy and the bloom was rotating counterclockwise, with two arms. High Ekman pumping velocity ($>4.5 \times 10^{-4}$ m s$^{-1}$) was estimated during the passage of Linfa (from 17 to 19 June). The monthly climatology of the mixed layer depth was about 20 m in June, and the maximum Ekman layer depth was about 346 m after Linfa. The analysis indicated that Linfa may have induced the cold eddy, where it looped around. With upwelling and entrainment, the eddy potentially provided nutrients to the bloom in the surface water. The results suggested that the sea surface current changes that Linfa induced had caused the bloom in an eddy feature. Tropical cyclones appear frequently in the SCS, which may affect the activities of mesoscale eddies in this area.



## 1. Introduction

The South China Sea (SCS) (3° 00′ – 23° 22′ N, 99° 10′ – 122° 10′ E), with a total area of about $3.5 \times 10^6$ km$^2$, is the largest semi-enclosed sea in the western tropical Pacific Ocean (figure 1) (Yang *et al.* 2002, Wang *et al.* 2009). It is also a cyclone-dominated tropical sea (Ren *et al.* 2002, Emanuel 2005, Zhou and Cui 2008). In the summer season, the northern SCS, which is generally stratified, tropical and oligotrophic, has low phytoplankton biomass (Ning *et al.* 2004, Zhao *et al.* 2009).

*Corresponding author. Email: lingzistdl@126.com

*International Journal of Remote Sensing*
ISSN 0143-1161 print/ISSN 1366-5901 online © 2012 Taylor & Francis
http://www.tandfonline.com
http://dx.doi.org/10.1080/01431161.2012.685976

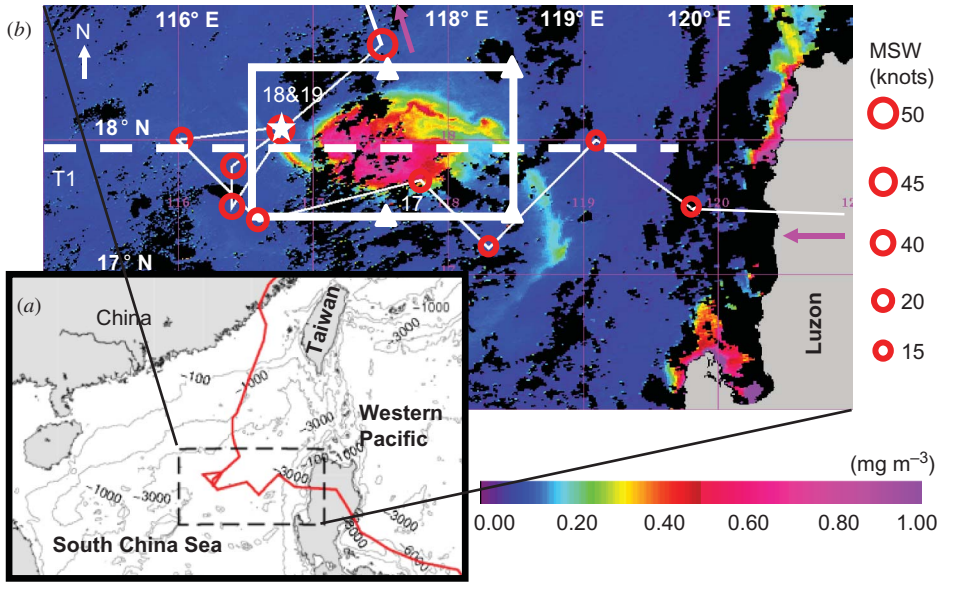


Figure 1. Geographic location and bathymetry of the study area (image *a*) and tropical cyclone centre positions and track (red lines) (circle diameter: maximum sustained wind speeds (1 knot = 0.514 m $s^{-1}$)). Image *b* is MODIS-derived sea surface chl-*a* concentration on 23 June 2009. Dates beside the cyclone centre show 00:00 UTC of each day. The white star shows the two-time passage over the same location at 00:00 UTC of 18 and 19 June. The white dashed line shows the location of the Ekman layer depths transect in figure 5. The white triangles show the location of the mixed layer depth data site.

Cold eddy vertical pumping of nutrients can fuel an eddy-feature phytoplankton bloom in the north-western Arabian Sea (Tang *et al.* 2002). Previous studies indicated that tropical cyclones can cause vertical mixing and upwelling and trigger an increase in chlorophyll (Price 1981, Subrahmanyam *et al.* 2002, Davis and Yan 2004, Chang *et al.* 2008). However, until now, there has been no observation of any phytoplankton bloom in an eddy feature that can reveal the dynamics of a cold eddy after a tropical cyclone. If we could find any linkage between an eddy-feature phytoplankton bloom and the cold eddy upwelling induced by a tropical cyclone, it would help us to better understand the impact of a tropical cyclone on phytoplankton.

Because the appearance of a tropical cyclone is always accompanied by thick clouds, it is difficult to identify information from satellite imagery. After having searched and analysed many cases of tropical cyclones using satellite remote-sensing data for the SCS, we finally seized on an opportunity to observe a phytoplankton bloom in an eddy-feature coinciding with the cold cyclonic eddy associated with a tropical cyclone in the SCS (figure 2(*c*)). We attempted to answer the question of how the phytoplankton bloom transformed into an eddy-featured bloom. This study provides some conclusive and fresh evidence of the relationships among tropical cyclones, cold eddies and eddy-feature phytoplankton blooms. It makes an advance in providing direct evidence for, and a comprehensive demonstration of, cold eddies and eddy-feature chlorophyll increases induced by tropical cyclones. This study can help us to improve our understanding of the mechanism of cold eddies and phytoplankton response to tropical cyclones.

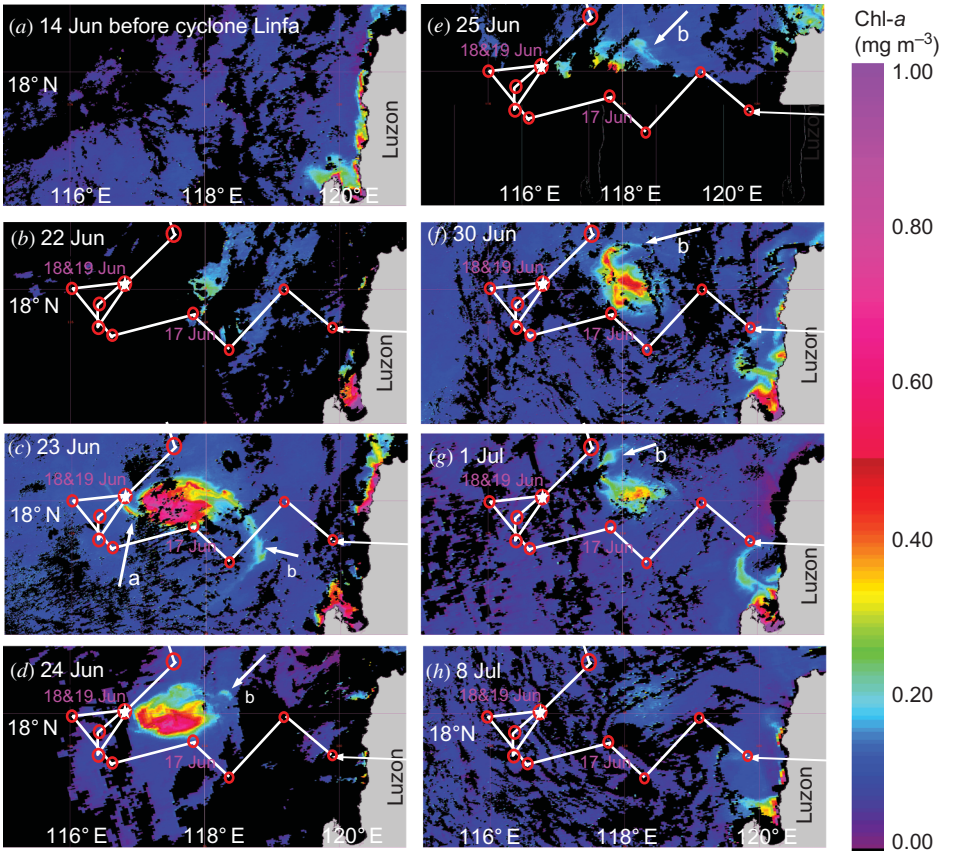


Figure 2. MODIS-derived sea surface chl-*a* concentration. (*a*) Before cyclone Linfa; (*b–g*) after cyclone Linfa. The white arrows show the dynamics of the arms around the bloom over the time. (The black areas indicate no data.)

## 2. Data and method

### 2.1 *Tropical cyclones and rainfall data*

In June 2009, category-1 (using the Saffir–Simpson tropical cyclone scale) tropical cyclone Linfa, which formed in the western Pacific, passed over the northern SCS (figure 1). Data for the cyclone's track and intensity evaluation were taken every 6 h and were used to identify the category of tropical cyclone Linfa. The cyclone track and study area were plotted using generic mapping tools (GMTs) (Wessel and Smith 1998) (figures 1 and 6). The cyclone-tracking data used in this study are available from the Unisys Weather website (http://weather.unisys.com) and are based on the best hurricane-track data issued from the Joint Typhoon Warning Center.

QuikScat wind speed data were produced by Remote Sensing Systems, sponsored by the NASA Ocean Vector Winds Science Team (available at www.remss.com).

Rainfall was estimated using TMPA-RT 3B42RT data with 0.25° × 0.25° spatial resolution. Daily precipitation regimes were provided by the TRMM (Tropical Rainfall Measuring Mission) Online Visualization and Analysis System (TOVAS), developed

by Goddard Earth Sciences (GES) and Distributed Active Archive Center (DAAC) (available at http://lake.nascom.nasa.gov/tovas).

### 2.2 *Sea surface temperature and chlorophyll-a concentration*

A new generation of global high-resolution (<10 km) sea surface temperature (SST) products was provided by the Group for High-Resolution SST (GHRSST). GHRSST L4 OSTIA data, with spatial resolutions of 5 km, used in the present study were provided by the Physical Oceanography Distributed Active Archive Center (PO.DAAC) Ocean Earth Science Information Partner (ESIP) Tool (POET), an interface developed by Ocean ESIP, a member of the ESIP Federation, under contract to NASA (available at poet.jpl.nasa.gov).

The Sea-viewing Wide Field-of-view Sensor (SeaWiFS) monthly climatology chlorophyll-*a* (chl-*a*) product with 9 km resolution and standard Level 2 products of the Moderate Resolution Imaging Spectroradiometer (MODIS) (1 km × 1 km) were provided by NASA's Ocean Color Working Group (available at http://oceancolor.gsfc.nasa.gov/) and were processed using the SeaWiFS Data Analysis System (SeaDAS) (Baith *et al.* 2001).

### 2.3 *Sea height anomalies and sea surface currents*

The near-real-time sea height anomalies (SHAs) and sea surface currents (SSCs) were derived from the JASON-1, TOPEX, European Remote Sensing-2 satellite (ERS-2), Environmental Satellite (ENVISAT) and Geodetic Satellite Follow-On (GFO) altimeters, processed by the Naval Research Laboratory (NRL) site at the Stennis Space Center; and the Global Telecommunication System (GTS) data were provided by National Oceanic and Atmospheric Administration/National Ocean Service (NOAA/NOS; available at www.aoml.noaa.gov). This field is derived from a 3 year global ocean model: Ocean Circulation and Climate Advanced Modelling project (OCCAM) run driven with realistic European Centre for Medium-Range Weather Forecasts (ECMWF) winds. The OCCAM mean sea surface height errors in boundary current separation regions are removed by using climatological dynamic heights based on Levitus (Kuroshio) and Lozier (Gulf Stream) climatologies (Fox *et al.* 2000).

### 2.4 *Ekman layer depth and Ekman pumping velocity*

Transect T1 (white dash line along 17.88° N in figure 1) (114.12°–120.12° E) across the upwelling region was designed for Ekman layer depth data sampling.

Daily mean Ekman layer depth can be calculated from the following equation (Stewart 2007):

$$D_{\mathrm{E}} = 7.12\,(\mathrm{sqrt}(\sin(\Phi)))^{-1} U_{10}, \tag{1}$$

where $D_{\mathrm{E}}$, $\phi$ and $U_{10}$ are, respectively, the Ekman layer depth, latitude and wind speed at 10 m above sea level. Previous studies showed that vertical mixing could reach a depth of 130 m, induced by Hurricane Fabian, in the vicinity of Bermuda (Black and Dickey 2008). In order to show the trend along transect T1 of the long-lasting tropical cyclone's effect on the upper ocean, we calculated the transient Ekman layer depth (the calculation neglects the effect of water-column stratification).

The Ekman pumping velocity was calculated from the following equation (Stewart 2007):

$$W_{\mathrm{E}} = -\mathrm{Curl}\left(T \times \rho^{-1} \times f^{-1}\right), \tag{2}$$

where $W_{\mathrm{E}}$ is the Ekman pumping velocity and $T$, $\rho$ and $f$ are, respectively, the wind stress, sea water density and the Coriolis parameter. Given the wind stress data, we obtained the Ekman pumping data from equation (2).

### 2.5 *Mixed layer depth*

The climatological monthly mean mixed layer depth fields were derived from the National Oceanographic Data Center. The data were computed from climatological monthly mean profiles of potential temperature based on temperature change from the ocean surface of 0.5°C (Monterey and Levitus 1997). Mixed layer depth was averaged from four sites (four white triangles in figure 1: 117.5° E, 17.5° N; 117.5° E, 18.5° N; 118.5° E, 17.5° N; and 118.5° E, 18.5° N) to reveal a background in the area in June.

## 3. Results

### 3.1 *Tropical cyclone Linfa*

Linfa was formed as a tropical depression in the deep interior of the north-west Pacific Ocean, with its centre located at 4.4° N, 139.6° E, at 00:00 UTC on 10 June 2009 (red line in figure 1). It moved north westwards first and passed over Luzon Island on 16 June. Thereafter, it headed westwards, entering the SCS. Linfa made two loops in three days (17–19 June) at approximately 18° N, 116.5° E, later changed its direction northward on the morning of 19 June, then intensified to a category-1 typhoon on 20 June and made landfall in the central coastal areas of Fujian Province on 21 June (red lines in figure 1).

Weak wind ($<7$ m s$^{-1}$) dominated in the northern SCS before Linfa's intrusion into the SCS (figure 3(*a*1)) from 7 to 13 June 2009, and high wind speed ($>30$ m s$^{-1}$) was observed on 19 June in the bloom area (figure 3(*a*2)).

### 3.2 *The eddy-feature phytoplankton bloom*

Chl-*a* concentrations were predominantly $<0.15$ mg m$^{-3}$ prior to the passage of the cyclone in the northern SCS (figures 2(*a*), 3(*c*1) and 4(*d*)). Large-scale cyclonic eddy-feature enhancement of chl-*a* concentration (chl-*a* $>$ 0.4 mg m$^{-3}$, indicating a phytoplankton bloom) was revealed by MODIS imagery (figures 2(*a*)–(*h*)) along the cyclone track, as compared to pre-cyclone chl-*a* concentration distribution. The bloom patch appeared between 160 and 440 km off the west coast of Luzon Island, where the depth was about 3500 m (figures 3(*d*2) and 6).

The bloom was first detected on 22 June (figure 2(*b*)); there were a few cloud-free pixels in image, but it could clearly show that the chl-*a* concentration had increased to a high value of 0.25 mg m$^{-3}$. The bloom showed a regular, elliptic cyclonic eddy feature with two arms (a and b) on 23 June (figures 2(*c*) and 3(*c*2)). The white arrows in figure 2 indicate the direction and feature changes of the bloom arms over time, showing cyclonic rotation of the bloom. The two arms are located at the 9 and 3 o'clock positions around the bloom (figure 2(*c*)) on 23 June. As time passed, chl-*a* data suggested

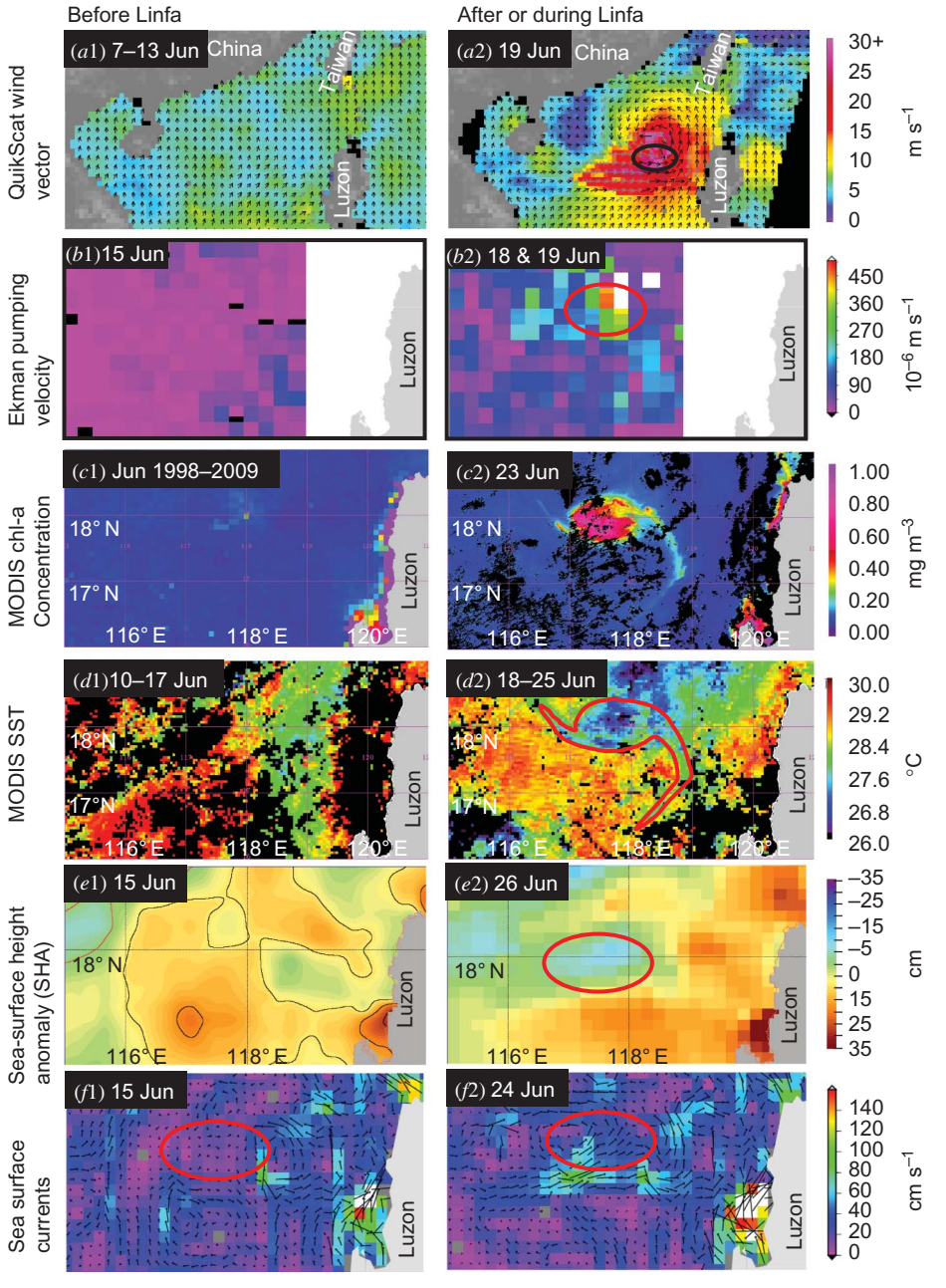


Figure 3. (*a*) Daily QuikScat wind-vector snapshots showing before (*a*1) and during (*a*2) Linfa (the black circle indicates the bloom area); (*b*) Ekman pumping velocities before (*b*1) and during (*b*2) tropical cyclone Linfa in the phytoplankton bloom area; (*c*) chl-*a* before (C1 shows the SeaWiFS monthly climatology chl-*a* product from June 1998–2009) and after (*c*2) Linfa; (*d*) sea-surface back ground (*d*1) and cooling (*d*2) in the region; (*e*) sea surface height anomaly (SHA) before (*e*1) and after (*e*2) Linfa; (*f*) Sea-surface currents before (*f*1) and after (SHA, *f*2) Linfa. (The black areas indicate no data.)

that arm a gradually disappeared and arm b rotated to the 2 o'clock position on 24 June (figure 2(*d*)), the 1 o'clock position on 25 June (figure 2(*e*)) and the 11 and then 10 o'clock positions on 30 June (figure 2(*f*)) and 1 July (figure 2(*g*)), respectively. The high chl-*a* concentration centre was located at 17.9° N, 117.45° E, on 23 June (figure 3(*c*2)). The area of chl-*a* concentration $>0.2$ mg m$^{-3}$ was about 8800 km$^2$. The high chl-*a* concentration patch was about 160 km in long-axis diameter and about 100 km in short-axis diameter on 23 June. Peak chl-*a* concentration of the bloom reached 6.7 mg m$^{-3}$ on 23 June.

### 3.3 *Cold eddy after the passage of cyclone Linfa*

Satellite-derived SST images clearly revealed a rapid cyclonic eddy feature; the location of the cold eddy was coincident with the maximum chl-*a* increase (figure 3(*c*2) and the red oval circle in *d*2). SST in the bloom area was high ($>$ 28°C) before the passage of tropical cyclone Linfa (figure 3(*d*1)). Tropical cyclone Linfa moved slowly from 17 to 19 June, and it took 3 days to complete two loops in the same place, where the phytoplankton bloom was detected on 22 June (figure 2(*b*)). SST images showing weak sea surface cooling appeared on 18 June, near 17.7° N, 118° E. This cooling was then enhanced on 19 June, reaching its lowest value of about 25°C on 20 June (figure not shown). The cold eddy lasted for 11 days (18–28 June) (figure 4(*d*)).

### 3.4 *Sea surface height and currents*

Multi-sensor (JASON-1, TOPEX, ERS-2, ENVISAT and GFO altimeters)-derived sea surface height and currents showed that the currents in the bloom area presented a anti-cyclonic shape (figure 3(*f*1)) before Linfa and changed to a cyclonic shape (figure 3(*f*2)) after Linfa, further suggesting the cyclonic cold eddy. Meanwhile, satellite-derived near-real-time altimeter images showed a low sea surface height anomaly (SHA) forming, which may be related to the upwelling that coincided with the chl-*a* patch in terms of location and time (24 June) – the lowest SHA value appearing on 26 June in the bloom region (red oval circle in figure 3(*e*2)). Furthermore, the eddy-feature phytoplankton bloom corresponded well to the SSCs after the passage of cyclone Linfa. The SSCs turned north (see the area marked by the area pointed out by the pink arrow in figure 6), where the chl-*a* concentration was high (figure 6).

### 3.5 *Time series data analysis*

To examine the variability in surface conditions, a time series of wind speed, TMPA-RT 3B42RT-derived rainfall, GHRSST and surface chl-*a* concentrations (MODIS) in the bloom area (white box in figure 1: 17.5°–18.5° N, 116.5°–118.5° E) and Ekman layer depth along transect T1 were analysed for the period from 14 June to 12 July 2009 (figure 4).

Wind speed reached a high value of 18.2 m s$^{-1}$ in the bloom area on 17 June. When the tropical cyclone strengthened, turning to a tropical storm on 19 June, the mean wind speed in the box area was about 18.5 m s$^{-1}$ (figure 4(*a*)).

The wind-induced Ekman layer depth in the box area showed high values ($>$230 m) on 17 and 18 June, revealed slightly reduced values from 19–22 June, after which the depth again reached high values on 23 June and reached the maximum depth on

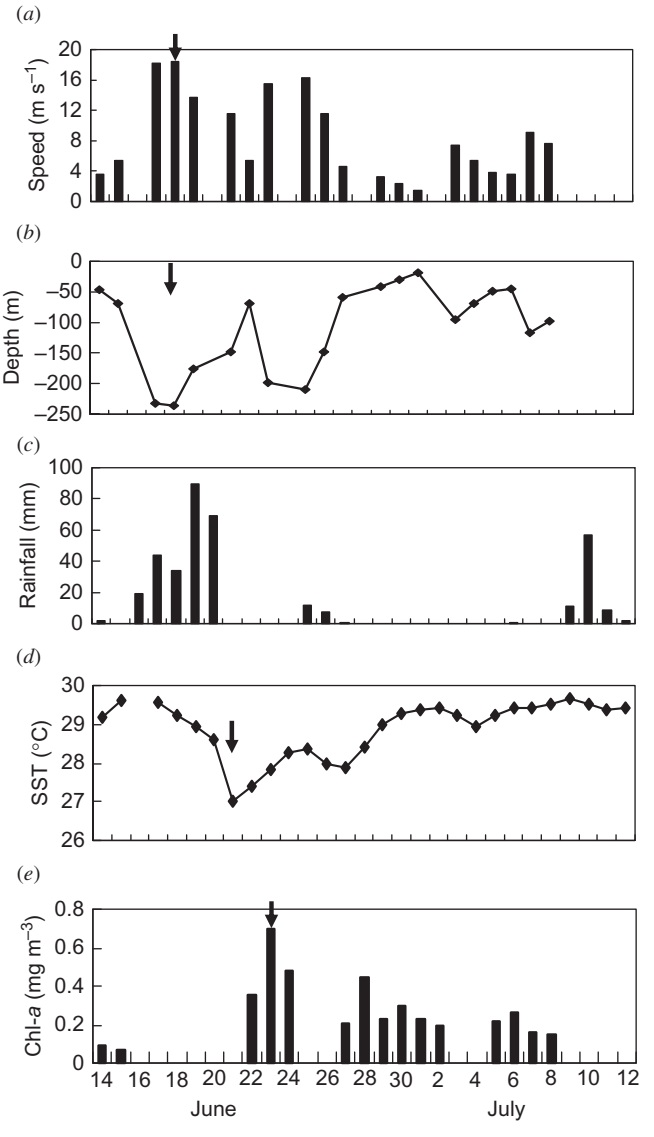


Figure 4. Time series observations in the bloom region (box in figure 1: 17.5°–18.5° N, 116.5°–118.5° E) during cyclone Linfa in late June and early July. Black arrows correspond to cyclone Linfa. (*a*) QuikScat mean daily wind speed; (*b*) Ekman layer depth; (*c*) TRMM-derived accumulated rainfall; (*d*) GHRSST, showing SST declined to the minimum on 21 June; (*e*) MODIS mean chl-*a* concentration.

25 June (figure 4(*b*)). The two maxima in the Ekman layer depth correspond to the two high wind speeds (figures 4(*a*) and (*b*)).

The rainfall rate was low (<20 mm day$^{-1}$) before the passage of tropical cyclone Linfa; it became high (89.26 mm day$^{-1}$ on 19 June) during the passage of the tropical cyclone. The rainfall rate increased to >4 times that of the pre-cyclone value (figure 4(*c*)).

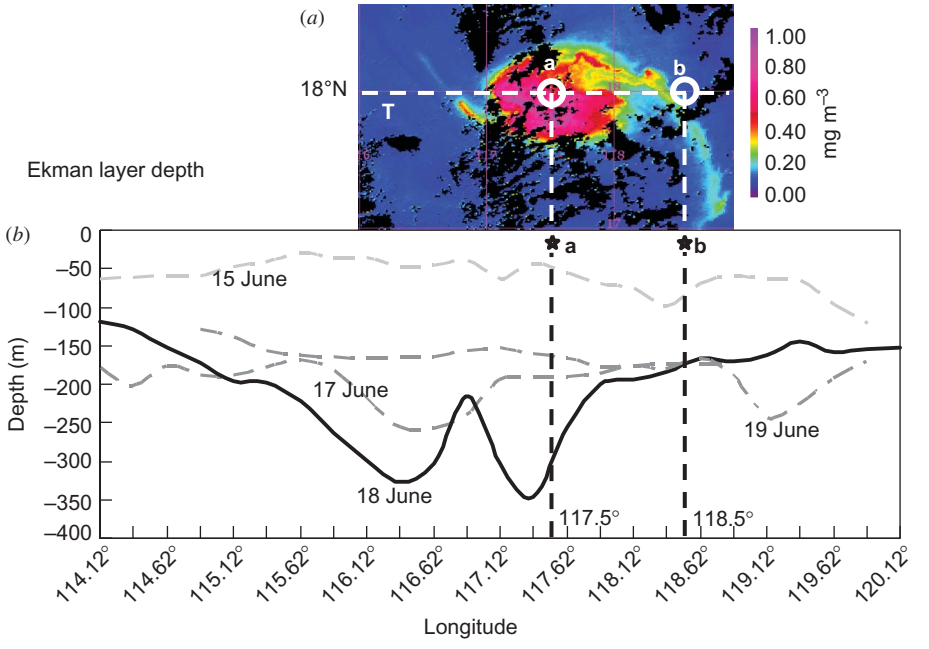


Figure 5. Depth of the Ekman layer depth along transect T1 (T in figure 1: 17.88° N, 114.12°–120.12° E) before (15 June) and during (17–19 June) tropical cyclone Linfa. Image *a* shows the geo-location of the two points (117.5° E, 18° N and 118.5° E, 18° N). The black stars (*a and *b) in image *b* show the mean monthly climatology of the mixed layer depth for the two points, respectively, in June.

SST decreased by about 1°C (from 29.55°C to 28.61°C) in the first three days after cyclone Linfa had passed and then rapidly decreased to 27.02°C, with maximum reduction (>2.5°C) on the fourth day (20 June, figure 4(*d*)).

Chl-*a* concentration increased to its maximum of 0.7 mg $m^{-3}$ on 23 June, 6 days after the passage of Linfa (black arrow in figure 4(*e*)), and reached another peak value (0.5 mg $m^{-3}$) on 28 June (white arrow in figure 4(*e*)).

### 3.6 *Ekman pumping, Ekman layer depth and mixed layer depth*

The Ekman pumping velocity displayed great changes: Ekman pumping was weak (figure 3(*b*1)) before tropical cyclone Linfa, but it appeared strong during cyclone Linfa (figure 3(*d*2)). Strong Ekman pumping appeared after the passage of tropical cyclone Linfa (figure 3(*d*2)); strong wind stress curls had induced seawater upwelling and had mainly contributed to the formation of the cyclonic cold eddy.

The wind-induced Ekman layer depth calculated along transect T1 is marked in figure 1 (white dashed line). Strong Ekman pumping mainly appeared on 17 and 18 June. The maximum depth of the Ekman layer reached 346.6 m on 18 June (figure 5). (Equation (1) neglects the effect of water-column stratification and the resulting estimates of Ekman layer depth are, at best, qualitative.)

The monthly climatology of the mixed layer depth was about 19.4 m in June (see *a and *b in figure 5). It showed that the background mixed layer depth was much shallow in non-typhoon situations.

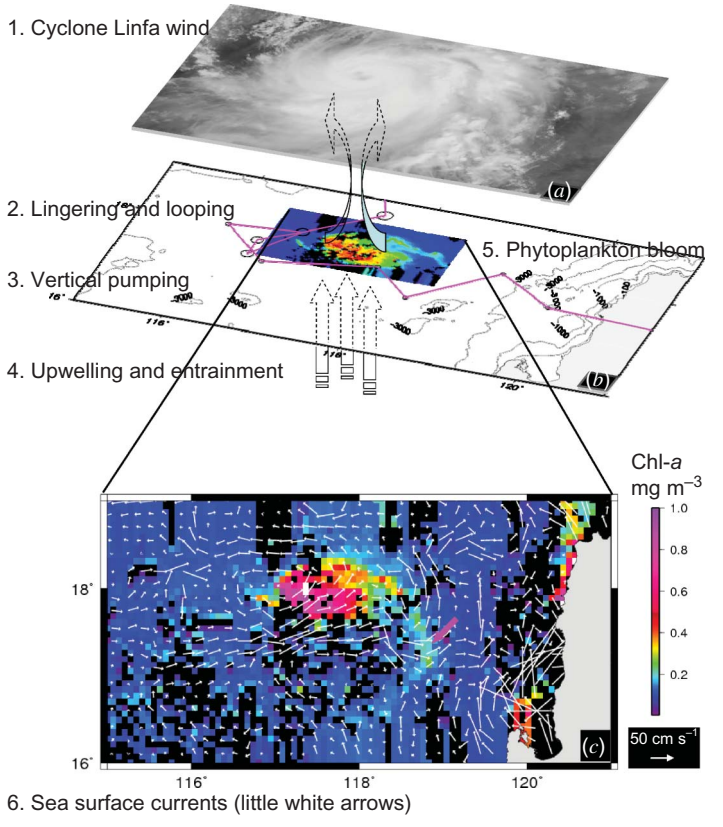


Figure 6. Mechanism of the eddy-feature chl-*a* bloom induced by the tropical cyclone in SCS. When tropical cyclone Linfa (1) made loops in the same location (2), Linfa induced strong vertical entrainment and upwelling (4) by vertical pumping (3), which supports nutrient for the eddy-feature chl-*a* bloom (5), and the sea surface currents changes after Linfa may lead to the chl-*a* bloom eddy feature (6). The pink line shows the tropical cyclone track while the pink arrow shows the northward turn of the sea surface currents.

## 4. Discussion

### 4.1 *Phytoplankton bloom in a cyclonic eddy feature*

A tropical cyclone can induce upwelling (Zheng and Tang 2007, Gierach and Subrahmanyam 2008) and a cold SST eddy can fuel a cyclonic eddy-feature phytoplankton bloom (Tang *et al.* 2002, Lee Chen *et al.* 2007). However, it is still necessary to clearly describe a cyclone-induced cyclonic eddy that supports eddy-feature phytoplankton blooms. The present study shows a good observation of a cyclonic eddy-feature phytoplankton bloom coincident with the cold cyclonic eddy's spiral structure. This observation implies that a tropical cyclone can induce cyclonic eddy upwelling and vertical entrainment. Furthermore, the eddy and entrainment provide nutrients to a phytoplankton bloom, giving it the cyclonic eddy feature (figure 6).

The northern SCS was dominated by high water temperature (>28°C) prior to cyclone Linfa (figures 3(*c*1) and 4(*b*)). After the passage of cyclone Linfa, a maximum sea surface cooling (3°C) patch appeared, coincident with the bloom's spiral structure along the track of Linfa (figures 3(*b*2) and (*d*2)). This study clearly showed an eddy

and eddy-feature bloom induced by a tropical cyclone, which may show some conclusive evidence of a relationship between the observed eddy-feature phytoplankton bloom and a tropical-cyclone-induced eddy upwelling.

The phytoplankton bloom showed a cyclonic eddy feature, which corresponded to the SSCs (figure 6). The correspondence of arm b of the phytoplankton bloom with the SSCs (pink arrow in figure 6) and the highest chl-*a* value to the highest currents indicated that the sea surface water currents lead the phytoplankton bloom to develop an eddy feature.

The anticlockwise rotation of the bloom arms (figures 2(*c*)–(*g*)) may reveal the movement of sea water over time (arrows in figure 2) and may further reveal the dynamics of the cyclonic eddy.



### 4.2 *Loop area for the phytoplankton bloom*

After tropical cyclones pass over the upper ocean with a long track, where do phytoplankton blooms usually occur? Previous studies indicated that the phytoplankton blooms in offshore deep oceans appeared in regions with stronger wind speeds and slower moving speeds during the passage of a tropical cyclone (Zhao *et al.* 2008). The present study detected a phytoplankton bloom in the region where the tropical cyclone made two loops and lingered for 3 days (figure 1), suggesting that the phytoplankton blooms tended to appear in the tropical cyclone looping and lingering area and could be matched well with an eddy feature (figures 1, 2(*b*) and 3(*b*2)).

The cooling of the SST after Linfa's passage showed that a tropical depression had triggered upwelling after it stayed in one place for more than 2 days. This may suggest that a tropical depression can induce upwelling and an increase in chlorophyll if it stayed and strengthened to a tropical storm in a region. There was high rainfall (figure 4(*b*)) during the tropical cyclone, which may have contributed somewhat to the SST's gradual decrease in the first few days after cyclone Linfa. This observation suggests that tropical cyclones can cause cyclonic eddies and eddy-feature phytoplankton blooms in the area where tropical cyclones loop and that a long duration of a tropical cyclone at a location is important for inducing phytoplankton bloom. In summary, the eddy-feature phytoplankton bloom is generated by the upwelling and entrainment induced by the long staying and looping of the tropical cyclone Linfa.

### 4.3 *Ekman pumping velocity, mixed layer depth and cyclonic eddy*

Ekman pumping velocity is an important index of vertical motions in oceans; it can help in understanding the distribution of chl-*a* in the study area (Stewart 2007, Zhao and Tang 2007). Our results revealed that the Ekman pumping velocity showed larger variability during cyclone Linfa (figure 3(*b*2)) than during the period before it (figure 3(*b*1)). The monthly mean mixed layer depth was about 19.4 m along transect T1 in June (figure 5), and this agreed well with the climatology of the mixed layer depth (about 20 m) for June in this area, which was estimated from individual profiles (De Boyer Montégut *et al.* 2004). In contrast to the mixed layer depth, the mean Ekman pumping layer depth was much thicker (218 m) after Linfa (figure 5). The increase in the mixed layer depth after the passage of Linfa may be due to the strong mixing of cyclones (Hung *et al.* 2010). The eddy-feature phytoplankton bloom was

caused by the combination of the 3 day looping and lingering of cyclone-induced upwelling.

Sea surface cooling, accompanied by a sea-level decrease (compared to the period before Linfa, figure 3(*e*1)), in the track of Linfa could indicate a cold cyclonic eddy upwelling (Zheng and Tang 2007) (figures 3(*c*2) and (*e*2)). The low SHA was detected on 24 June, one day after the appearance of the cyclonic eddy-feature chl-*a* bloom on 23 June (figure 3(*b*2)). It is well known that the SCS is a tropical, cyclone-dominated tropical sea (Zheng and Tang 2007), and it is also a mesoscale eddy-active region (Su 2004, Liu *et al.* 2008). Generally, a mesoscale phenomenon's dimensional scale is in the tens to hundreds of kilometres and the time frame is in days to months (Li 2002, Wang *et al.* 2005). Wind stress curl can stimulate mesoscale eddies (Chu *et al.* 1998). The cyclonic eddy observed in the present study, induced by Linfa, presenting for about 11 days and spanning an area of about $1^\circ \times 1.5^\circ$, could be considered a mesoscale eddy. Therefore, tropical cyclones may make a contribution to enhancing mesoscale eddies in the SCS. This calls for more observation and investigation.

## 5. Summary

The eddy-feature phytoplankton bloom was fuelled by the vertical entrainment and upwelling induced by the lingering and looping of a tropical cyclone (figure 6). The lingering and looping of a tropical cyclone can cause strong Ekman pumping and strong mixing of ocean water (figure 3(*b*2)), which nourishes the eddy-feature phytoplankton bloom. The cyclonic eddy-feature phytoplankton bloom was generated where the tropical cyclone had stayed for a long time and looped around. The eddy-feature phytoplankton bloom corresponded to the SSCs, suggesting that the SSC changes induced by the tropical cyclone had led to the phytoplankton bloom in a cyclonic eddy feature.

The anticlockwise rotation of the bloom arms (figure 2) may give us a view of the movement of the cyclone-induced cold eddy waters. This may help us to better understand the motion of cold eddies.

The long staying and looping of tropical cyclones provided a positive effect on inducing phytoplankton bloom. Tropical cyclones may have a positive effect on the enhancement of mesoscale eddies in the SCS.

**Acknowledgements**

The present research was supported by the following grants awarded to D. Tang: (1) National Natural Science Foundation of China (40976091, 31061160190 and 40811140533); (2) Chinese Academy of Sciences (kzcx2-yw-226); (3) the CAS/SAFEA International Partnership Programme for Creative Research Teams (KZCX2-YW-T001 and KZCX2-YW-213); (4) Guangdong Natural Science Foundation, China (8351030101000002). NASA's Ocean Color Working group provided the MODIS data. Remote Sensing Systems provided the QuikScat wind-vector data. The Physical Oceanography Distributed Active Archive Center (PO.DAAC) provided the GHRSST and QuikScat wind speed data. We thank Dr Gad Levy of North West Research Associates, USA, Ms Pauline Lovell and Ms Stephanie King for their comments on the manuscript.

## References


Baith, K., Lindsay, R., Fu, G. and McClain, C.R., 2001, SeaDAS: data analysis system developed for ocean color satellite sensors. *EOS Transactions American Geophysical Union*, **82**, pp. 202–205.

Black, W.J. and Dickey, T.D., 2008, Observations and analyses of upper ocean responses to tropical storms and hurricanes in the vicinity of Bermuda. *Journal of Geophysical Research*, **113**, C08009, doi:10.1029/2007JC004358.

Chang, Y., Liao, H.-T., Lee, M.-A., Chan, J.-W., Shieh, W.-J., Lee, K.-T., Wang, G.-H. and Lan, Y.-C., 2008, Multisatellite observation on upwelling after the passage of Typhoon Hai-Tang in the southern East China Sea. *Geophysical Research Letters*, **35**, L03612, doi:10.1029/2007GL032858.

Chu, P.C., Fan, C., Lozano, C.J. and Kerling, J.L., 1998, An airborne expendable bathythermograph survey of the South China Sea, May 1995. *Journal of Geophysical Research*, **103**, pp. 21637–21652.

Davis, A. and Yan, X.H., 2004, Hurricane forcing on chlorophyll-a concentration off the northeast coast of the U.S. *Geophysical Research Letters*, **31**, L17304, doi:10.1029/2004GL020668.

De Boyer Montégut, C., Madec, G., Fischer, A.S., Lazar, A. and Iudicone, D., 2004, Mixed layer depth over the global ocean: an examination of profile data and a profile-based climatology. *Journal of Geophysical. Research*, **109**, C12003, doi:10.1029/2004JC002378.

Emanuel, K., 2005, Increasing destructiveness of tropical cyclones over the past 30 years. *Nature*, **436**, pp. 686–688.

Fox, A., Keith, H., Beverley, D.C. and Webb, D., 2000, Altimeter assimilation in the OCCAM Global Model, Part II: TOPEX/POSEIDON and ERS1 data. *Journal of Marine Systems*, **26**, pp. 323–347.

Gierach, M.M. and Subrahmanyam, B., 2008, Biophysical responses of the upper ocean to major Gulf of Mexico hurricanes in 2005. *Journal of Geophysical Research*, **113**, C04029, doi:10.1029/2007JC004419.

Hung, C.-C., Gong, G.-C., Chou, W.-C., Chung, C.-C., Lee, M.-A., Chang, Y., Chen, H.-Y., Huang, S.-J., Yang, Y., Yang, W.-R., Chung, W.-C., Li, S.-L. and Laws, E., 2010, The effect of typhoon on particulate organic carbon flux in the southern East China Sea. *Biogeosciences*, **7**, pp. 3007–3018.

Lee Chen, Y.L., Chen, H.Y., Lin, I.I., Lee, M.A. and Chang, J., 2007, Effects of cold Eddy on phytoplankton production and assemblages in Luzon Strait bordering the South China Sea. *Journal of Oceanography*, **63**, pp. 671–683.

Li, L., 2002, A review on mesoscale oceanographical phenomena in the South China Sea. *Journal of Oceanography in Taiwan Strait*, **21**, pp. 265–274 [in Chinese].

Liu, Q.Y., Kaneko, A. and Su, J.L., 2008, Recent progress in studies of the South China Sea circulation. *Journal of Oceanography*, **64**, pp. 753–762.

Monterey, G. and Levitus, S., 1997, *Seasonal Variability of Mixed Layer Depth for the World Ocean, NOAA Atlas NESDIS 14*, 96 p. (Washington, DC: U.S. Government Printing Office).

Ning, X., Chai, F., Xue, H., Cai, Y., Liu, C. and Shi, J., 2004, Physical-biological oceanographic coupling influencing phytoplankton and primary production in the South China Sea. *Journal of Geophysical Research*, **109**, C10005, doi:10.1029/2004JC002365.

Price, J.F., 1981, Upper ocean response to a hurricane. *Journal of Physical Oceanography*, **11**, pp. 153–175.

Ren, F., Gleason, B. and Easterling, D., 2002, Typhoon impacts on China's precipitation during 1957–1996. *Advances in Atmospheric Sciences*, **19**, pp. 943–952.

Stewart, R.H., 2007, Response of the upper ocean to winds. Available online at: http://oceanworld.tamu.edu/resources/ocng_textbook/contents.html (accessed 20 November 2009).

Su, J.L., 2004, Overview of the South China Sea circulation and its influence on the coastal physical oceanography outside the Pearl River Estuary. *Continental Shelf Research*, **24**, pp. 1745–1760.

Subrahmanyam, B., Rao, K.H., Rao, N.S., Murty, V.S.N. and Sharp, R.J., 2002, Influence of a tropical cyclone on chlorophyll-*a* concentration in the Arabian Sea. *Geophysical Research Letters*, **29**, 2051, doi:10.1029/2002GL015892.

Tang, D.L., Kawamura, H. and Luis, A.J., 2002, Short-term variability of phytoplankton blooms associated with a cold eddy in the northwestern Arabian Sea. *Remote Sensing of Environment*, **81**, pp. 82–89.

Wang, G.H., Ling, Z. and Wang, C., 2009, Influence of tropical cyclones on seasonal ocean circulation in the South China Sea. *Journal of Geophysical Research*, **114**, C10022, doi:10.1029/2009JC005302.

Wang, G.H., Su, J.L. and Qi, Y.Q., 2005, Advances in studying Mesoscale Eddies in South China Sea. *Advances in Earth Science*, **20**, pp. 882–886 [in Chinese].

Wessel, P. and Smith, W.H.F., 1998, New improved version of the generic mapping tools released. *EOS Transactions American Geophysical Union*, **79**, p. 579.

Yang, H.J., Liu, Q.Y., Liu, Z.Y., Wang, D.X. and Liu, X.B., 2002, A general circulation model study of the dynamics of the upper ocean circulation of the South China Sea. *Journal of Geophysical Research*, **107**, 3085, doi:10.1029/2001JC001084.

Zhao, H. and Tang, D.L., 2007, Effect of 1998 El Nin∼o on the distribution of phytoplankton in the South China Sea. *Journal of Geophysical Research*, **112**, C02017, doi:10.1029/2006JC003536.

Zhao, H., Tang, D.L. and Wang, D.X., 2009, Phytoplankton blooms near the Pearl River Estuary induced by Typhoon Nuri. *Journal of Geophysical Research*, **114**, C12027, doi:10.1029/2009JC005384.

Zhao, H., Tang, D.L. and Wang, Y., 2008, Comparison of phytoplankton blooms triggered by two typhoons with different intensities and translation speeds in the South China Sea. *Marine Ecology Progress Series*, **365**, pp. 57–65.

Zheng, G.M. and Tang, D.L., 2007, Offshore and nearshore chlorophyll increases induced by typhoon winds and subsequent terrestrial rainwater runoff. *Marine Ecology Progress Series*, **333**, pp. 61–72.

Zhou, B. and Cui, X., 2008, Hadley circulation signal in the tropical cyclone frequency over the western North Pacific. *Journal of Geophysical Research*, **113**, D16107, doi:10.1029/2007JD009156.